Int. J. Heat Mass Transfer. Vol. 28, No. 12, pp. 2379–2382, 1985
Printed in Great Britain

0017–9310/85 $3.00 + 0.00

TECHNICAL NOTES

Finned-tube performance evaluations for one-row arrays and two-row staggered and in-line arrays

F. SAMIE* and E. M. SPARROW
Department of Mechanical Engineering, University of Minnesota, Minneapolis, MN 55455, U.S.A.

(*Received* 2 *March* 1985 *and in final form* 11 *June* 1985)

INTRODUCTION

IN THIS paper, performance evaluations are carried out for the one- and two-row arrays of annular fins for which basic heat transfer and pressure drop data were obtained in [1]. For the one-row arrays, both the per-tube Nusselt number and the array pressure drop were found to increase with decreasing transverse pitch, thereby precluding the intuitive selection of an optimum pitch. Similarly, for the two-row arrays, both the Nusselt number and the pressure drop were higher when the tubes were deployed in a staggered pattern than in an in-line pattern, making it difficult to choose between the staggered and in-line deployments. Here, performance-related criteria will be utilized for the selection of the optimum transverse pitch for the one-row arrays and for the staggered vs in-line decision for the two-row arrays. The two criteria to be used are: (1) the maximization of the heat transfer rate for a given pumping power and (2) the maximization of the heat transfer rate for a given pressure drop.

In the forthcoming description of the analysis, familiarity with the contents and nomenclature of [1] will be assumed. The layouts of the arrays to be investigated are illustrated in Fig. 2 of [1].

ONE-ROW ARRAYS

In addition to the aforementioned fixed pumping power and fixed pressure drop conditions, two geometrical conditions will be considered in the performance analysis of the one-row arrays. One of these is that the number of tubes in the array is fixed, so that the transverse width of the heat exchanger varies in response to changes in the transverse pitch. The second is that the transverse width of the heat exchanger is fixed, which requires that the number of tubes in the array changes as the transverse pitch changes.

In assessing the performance of the various one-row arrays (i.e. corresponding to variations of the transverse pitch), it is convenient to select one of the pitches as a base case and to compare the others with it. For concreteness, the smallest of the investigated pitches, $S_T/D_f = 1.07$, will be used for the base case and will be designated by an asterisk.

Fixed number of tubes

The first focus of the analysis is to determine the heat transfer response to variations of the transverse pitch at a fixed pumping power. If Δp is the pressure drop across the array and $\dot{m}$ is the mass flowrate, then the pumping power P is given by

$$P = (\dot{m}/\rho)\,\Delta p. \tag{1}$$

For a row of N tubes (each of length L) deployed with a transverse pitch S_T, the rate of flow through the array is $\dot{m} = N[\rho(LS_T)U_\infty]$. In [1], the pressure drop was represented in dimensionless terms by the pressure loss coefficient $K_{p\infty} = \Delta p/\frac{1}{2}\rho U_\infty^2$. Upon elimination of $\dot{m}$ and Δp from equation (1) and introducing the Reynolds number $Re_\infty = \rho U_\infty D/\mu$, there follows

$$P' \equiv P[2\rho^2 D^3/ND_f L\mu^3] = (S_T/D_f)K_{p\infty}Re_\infty^3. \tag{2}$$

* Present address: General Motors Research Laboratories, Warren, Michigan, U.S.A.

NOMENCLATURE

A_b	exposed area of base tube
A_f	fin surface area (annular faces and tips)
D	diameter of base tube
D_f	diameter of fin tips
h	per-tube heat transfer coefficient
$K_{p\infty}$	pressure loss coefficient
k	thermal conductivity
L	tube length
$\dot{m}$	mass flowrate through array
N	number of tubes
Nu	per-tube Nusselt number
P	pumping power
Pr	Prandtl number
Δp	array pressure drop
Q	array heat transfer rate
Q_I	heat transfer rate for in-line array
Q_S	heat transfer rate for staggered array
Q^*	heat transfer rate for base case
Re_∞	freestream Reynolds number, $\rho U_\infty D/\mu$
$Re_{\infty,I}$	Reynolds number for in-line array
$Re_{\infty,S}$	Reynolds number for staggered array
Re_∞^*	Reynolds number for base case
S_L	longitudinal pitch
S_T	transverse pitch
T_b	base tube temperature
T_{mix}	mixed-mean temperature
T_x	temperature of air approaching second row
T_∞	freestream temperature upstream of array
U_∞	freestream velocity upstream of array
W	width of heat exchanger.

Greek symbols

η	fin efficiency
μ	viscosity
ρ	density.

Other symbols

$\bar{}$	circumferential average.

The quantity in brackets which multiplies P is a constant, so that the fixed pumping power condition can be imposed by requiring that P' be fixed.

Since $K_{p\infty}$ is a function of S_T/D_f and Re_∞ (Fig. 10 of [1]), a graph can be prepared in which P' is plotted vs Re_∞ for parametric values of S_T/D_f. Then, a value of P' is selected, and the Re_∞ which yields that value of P' can be read off for each S_T/D_f. As expected, such a procedure shows that the fulfillment of the fixed pumping power condition requires that Re_∞ decrease with decreasing S_T/D_f.

To systematically select the fixed values of P' at which to make the performance comparison, rounded values of the base case Reynolds number Re^*_∞ (i.e. Re_∞ values for $S_T/D_f = 1.07$) are chosen and the corresponding P' values are read from the aforementioned graph. Once a P' is established, the Re_∞ values for all of the pitches are read off. Thus, for each Re^*_∞, there is a set of Re_∞ values, which depend on S_T/D_f, that yield the same pumping power P'.

Next, turning to the rate of heat transfer Q, it follows directly from [1] that for an array of N tubes,

$$Q = N[h(A_b + \eta A_f)(\overline{T_b - T_\infty})] \tag{3}$$

in which, on a per-tube basis, A_b is the exposed surface area of the base tube, and A_f is the fin surface area, including the annular faces and the tips. The temperatures T_b and T_∞ respectively correspond to the base tube and to the freestream approaching the array, and $(\overline{T_b - T_\infty})$ is the circumferential-average temperature difference.

Equation (3) may be used to compare the rate of heat transfer for an arbitrary case to that for the base case, so that

$$Q/Q^* = [(A_b + \eta A_f)Nu]/[(A_b + \eta A_f)Nu]^*. \tag{4}$$

Both the Nusselt number Nu and the fin efficiency η depend on Re_∞ and S_T/D_f, but, for η, the dependence is slight and, in general, η does not deviate very much from unity.

For the selected Re^*_∞ (i.e. for $S_T/D_f = 1.07$), Nu and η can be obtained from [1], as can the Nu and η values for the Re_∞, S_T/D_f pairs which correspond to the same pumping power as the selected Re^*_∞. Thus, Q/Q^* can be evaluated as a function of S_T/D_f for the fixed pumping power condition, and these results will be presented shortly.

The analysis to determine the heat transfer response to variations of the transverse pitch at a fixed pressure drop follows a path very similar to that just described for the fixed pumping power condition. From the definition of the pressure loss coefficient $K_{p\infty}$, a rephrasing yields

$$\Delta p' \equiv \Delta p[2\rho D^2/\mu^2] = K_{p\infty} Re^2_\infty. \tag{5}$$

A fixed value of Δp is equivalent to a fixed value of $\Delta p'$, since the bracketed quantity is constant. By using the $K_{p\infty}$ vs Re_∞ information from [1], a graph can be constructed in which $\Delta p'$ is plotted as a function of Re_∞ for parametric values of S_T/D_f.

Equation (5) plays a role in the fixed pressure drop analysis that is completely analogous to that played by equation (2) in the fixed pumping power analysis. All of the steps in the analysis which follow equation (2) can also be carried out using equation (5) as a basis. The end result is the variation of Q/Q^* as a function of S_T/D_f for the fixed pressure drop condition.

The Q/Q^* vs S_T/D_f results are presented in Figs. 1(a) and (b) for the fixed pumping power and fixed pressure drop conditions, respectively. The results are parameterized by two values of Re^*_∞, which serve either to specify two fixed values of the pumping power or two fixed values of the pressure drop. Note that $Q/Q^* = 1$ when $S_T/D_f = 1.07$ for both conditions, as is consistent with the selection of this pitch as the base case.

Considering Fig. 1(a), it is seen that at a fixed pumping power and a fixed number of tubes, the rate of heat transfer is very little affected by the transverse pitch for both of the selected Re^*_∞. On the other hand, for a fixed pressure drop and a fixed number of tubes, the heat transfer rate increases significantly with increasing values of the transverse pitch, as can be seen in Fig. 1(b). Since the width of the heat exchanger is

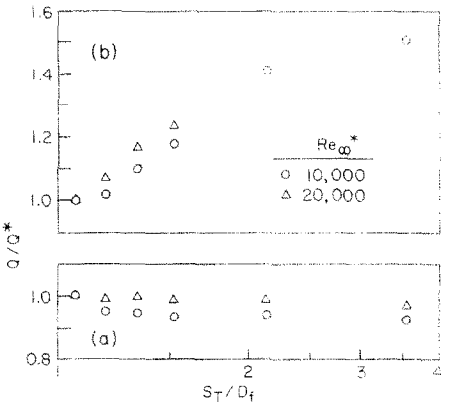

FIG. 1. Heat transfer response to transverse pitch for one-row heat exchangers having a fixed number of tubes: (a) fixed pumping power; (b) fixed pressure drop.

equal to NS_T, the pitch-related increase in the heat transfer requires the use of a wider heat exchanger, which, in applications where space is constrained, may not be permissible.

Fixed heat exchanger width

The performance analysis for one-row, fixed-width heat exchangers is most readily carried out by modifying the foregoing analysis for one-row heat exchangers having a fixed number of tubes. Since the width W is equal to NS_T and W is fixed, it follows that the number of tubes N is equal to W/S_T.

For the fixed pumping power condition, the fact that the NS_T product is a constant can be incorporated into equation (2), yielding

$$P'' \equiv P[2\rho^2 D^3/WL\mu^3] = K_{p\infty} Re^3_\infty. \tag{6}$$

From this equation, it is seen that the fixed pumping power condition is now equivalent to $P'' =$ constant. Thus, the entire discussion of the use of equation (2) also applies here merely by substituting P'' for P'. Furthermore, upon taking account of the fact that N varies with S_T, equation (4) for the heat transfer ratio becomes

$$Q/Q^* = [N(A_b + \eta A_f)Nu]/[N(A_b + \eta A_f)Nu]^* \tag{7}$$

where $N/N^* = S^*_T/S_T$. Equations (6) and (7) can be used to generate the variation of Q/Q^* with S_T/D_f for the fixed pumping power condition.

For the fixed pressure drop condition, equation (5) continues to apply without modification, and it is used together with equation (7) to compute Q/Q^* as a function of S_T/D_f.

The Q/Q^* results for the fixed width condition are presented in Figs. 2(a) and (b). The (a) part of the figure is for fixed pumping power and is referred to the left-hand ordinate for Q/Q^*, while the (b) part is for fixed pressure drop and is referred to the right-hand ordinate for Q/Q^*. Both parts share the same abscissa for S_T/D_f. In each part, results are plotted for two values of Re^*_∞, which represent either two fixed values of the pumping power or two fixed values of the pressure drop.

As seen in the figure, the results for both the fixed pumping power condition and the fixed pressure drop condition display the same trend, which is also common to the two selected values of Re^*_∞. The figure shows that the largest value of Q/Q^* corresponds to the smallest of the investigated transverse pitches (i.e. $S_T/D_f = 1.07$) and that Q/Q^* decreases monotonically with increasing pitch. Thus, for a fixed heat exchanger width, the rate of heat transfer is maximized by using as many tubes as possible, and this conclusion applies for both the fixed pumping power condition and the fixed pressure drop condition.

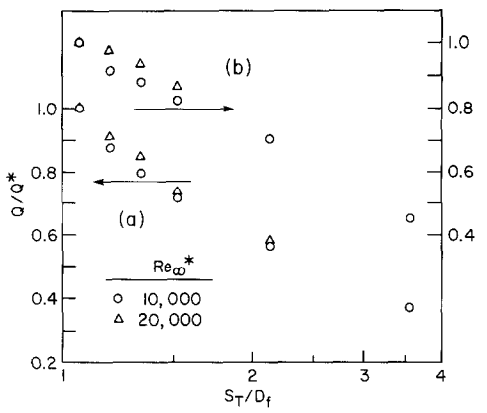

FIG. 2. Heat transfer response to transverse pitch for one-row, fixed-width heat exchangers: (a) fixed pumping power; (b) fixed pressure drop.

TWO-ROW ARRAYS

The issue to be considered for the two-row arrays is the choice between staggered and in-line deployment of the tubes. Comparisons of the two types of deployments will be made for a fixed, practically-relevant value of the transverse pitch (i.e. $S_T/D_f = 1.52$), for a fixed number of tubes in each row, and for each of two longitudinal pitches in the practical range ($S_L/D_f = 1.26$ and 1.52).

If $K_{p\infty}$ now represents the pressure loss coefficient for a two-row array, the fixed pumping power condition is expressed by equation (6), since the aforementioned fixed S_T and fixed number of tubes imply a fixed heat exchanger width. Equation (6) was used to establish the correspondence between the staggered-array Reynolds numbers $Re_{\infty,S}$ and in-line-array Reynolds numbers $Re_{\infty,I}$ which fulfill the fixed pumping power condition. Using the $K_{p\infty}$ data from Fig. 12 of [1] in conjunction with equation (6), graphs were prepared for the staggered and in-line arrays, respectively, in which P'' was plotted vs Re_∞ for the two parametric values of S_L/D_f. Then, for selected values of $Re_{\infty,S}$ and S_L/D_f, P'' was read from the graph for the staggered case. This P'' was then used as input to the graph for the in-line case, and the value of $Re_{\infty,I}$ corresponding to the preselected S_L/D_f was read off. This procedure was carried out for a succession of $Re_{\infty,S}$ values for each of the S_L/D_f.

For the fixed pressure drop condition, equation (5) continues to apply provided that $K_{p\infty}$ is now understood to be the pressure loss coefficient for a two-row array. In a manner similar to that of the preceding paragraph, equation (5) was used to determine the correspondence between $Re_{\infty,S}$ and $Re_{\infty,I}$ values which fulfill the fixed pressure drop constraint.

Attention is now turned to the heat transfer analysis. For the two-row array,

$$Q = Q_1 + Q_2 \tag{8}$$

where Q_1 and Q_2 represent the rates of heat transfer at the tubes in the first and second rows, respectively. For the evaluation of Q_1 and Q_2, it is relevant to note that the experiments reported in [1] were performed with only one heated tube in the array, either situated in the first row or in the second row. On the other hand, the Q that is being sought in equation (8) is for all tubes thermally active and having the same base tube temperature T_b ($> T_\infty$).

For Q_1, it is believed that the expression

$$Q_1 = [Nh(A_b + \eta A_f)(\overline{T_b - T_\infty})]_1 \tag{9}$$

provides accurate heat transfer rates even when both rows are thermally active. However, for Q_2, it is necessary to take account of the possible temperature elevation of the air which arrives at the second row when there is heating in the first row. If T_x denotes the temperature of the air between the rows, then Q_2 will be expressed as

$$Q_2 = [Nh(A_b + \eta A_f)(\overline{T_b - T_x})]_2. \tag{10}$$

Two models will be used for T_x. First, by setting $T_x = T_\infty$, an upper bound is obtained for Q_2 and, therefore, for Q. In that case, equations (8)–(10) become

$$Q[D/Nk(\overline{T_b - T_\infty})] = [(A_b + \eta A_f)\,Nu]_1 + [(A_b + \eta A_f)\,Nu]_2. \tag{11}$$

In the second model, the air is assumed to be perfectly mixed subsequent to its thermal interaction with the first row, so that

$$N[\rho(LS_T)U_\infty]c_p(T_x - T_\infty) = Q_1. \tag{12}$$

The T_x ($\equiv T_{mix}$) determined by solving equation (12) in conjunction with equation (9) yields an expression for Q which differs from equation (11) in that the second bracketed term on the RHS is multiplied by the factor

$$1 - [(A_b + \eta A_f)\,Nu]_1/Re\,Pr\,LS_T \tag{13}$$

which is always less than unity.

By using the $Re_{\infty,I}$, $Re_{\infty,S}$ pairs consistent with either the fixed pumping power condition or the fixed pressure drop condition, equation (11) or its modified form [i.e. the multiplying factor in equation (13)] can be evaluated to yield the ratio Q_I/Q_S. The numerical results for the Q_I/Q_S ratio are plotted in Fig. 3 as a function of $Re_{\infty,S}$ for both the fixed pumping power and fixed pressure drop conditions, for the two longitudinal pitches $S_L/D_f = 1.26$ and 1.52, and for the $T_x = T_\infty$ and $T_x = T_{mix}$ models. To provide continuity, lines have been faired through the fixed pumping power results and the fixed pressure drop results, respectively.

The main message of the figure is that the in-line-array heat transfer is greater than the staggered-array heat transfer. For the fixed pumping power condition, Q_I exceeds Q_S by 4–12%,

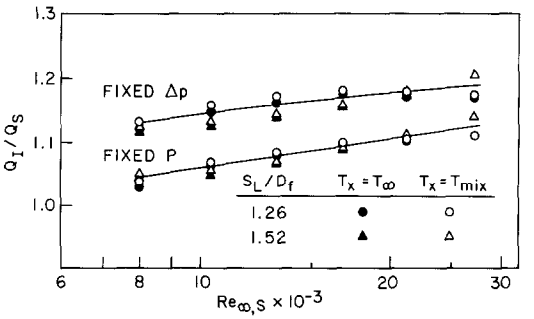

FIG. 3. Heat transfer comparisons for two-row, in-line and staggered arrays.

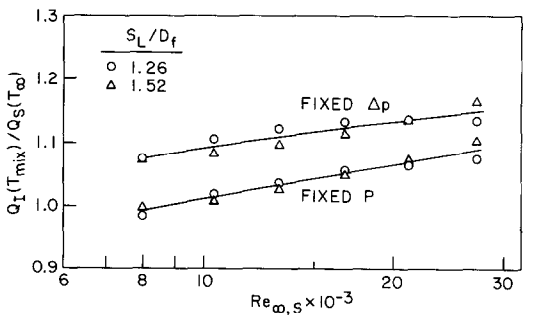

FIG. 4. Alternative heat transfer comparisons for two-row, in-line and staggered arrays.

depending on the Reynolds number, while the corresponding differences are 13–19% for the fixed pressure drop condition. The weak dependence of the results on S_L/D_f suggests that they can be regarded as universal (i.e. independent of S_L/D_f) in the investigated range.

The near coincidence of the Q_I/Q_S values for the $T_x = T_\infty$ and $T_x = T_{mix}$ models appears to lend credence to the superior performance of the in-line array. However, it can be argued that both models are unfair to the staggered array. To neutralize this concern, Q_I corresponding to the $T_x = T_{mix}$ model will be compared to Q_S for the $T_x = T_\infty$ model, thereby penalizing the in-line array since $(\overline{T_b - T_{mix}})$ is smaller than $(\overline{T_b - T_\infty})$. The ratio $Q_I(T_{mix})/Q_S(T_\infty)$ is plotted in Fig. 4. Although the Q ratios in Fig. 4 are closer to unity than those of Fig. 3, Q_I continues to exceed Q_S. Thus, for the investigated cases, it appears advantageous to use in-line deployment in preference to staggered deployment.

REFERENCE

1. E. M. Sparrow and F. Samie, Heat transfer and pressure drop results for one- and two-row arrays of finned tubes, *Int. J. Heat Mass Transfer* **28**, 2247–2259 (1985).

Int. J. Heat Mass Transfer. Vol. 28, No. 12, pp. 2382–2385, 1985
Printed in Great Britain

0017-9310/85 $3.00 + 0.00

Countercurrent flow limits for steam and cold water through a horizontal perforated plate with vertical jet injection*

I. DILBER and S. G. BANKOFF†
Chemical Engineering Department and Mechanical and Nuclear Engineering Department, Northwestern University, Evanston, IL 60201, U.S.A.

(*Received* 15 *August* 1984 *and in final form* 28 *May* 1985)

INTRODUCTION

IN A POSTULATED loss-of-coolant accident in a light-water nuclear reactor, emergency core cooling system water may be injected into the upper plenum above the upper tie plate. However, penetration of this water downwards into the core can occur only when the steam rising from the overheated core drops below a critical flooding velocity. This flooding phenomenon has been studied in various geometries [1, 2]. Bankoff *et al.* [3] determined the points of zero and complete water delivery for steam–water and air–water countercurrent flow through horizontal perforated plates, using a horizontal spray for the injected water. The present study is an extension of this work, in which a vertically downwards water jet at various elevations above the plate is employed. Significantly increased penetration capabilities are found, pointing towards the possibility of improved core cooling and lower peak clad temperatures.

EQUIPMENT AND PROCEDURE

The equipment, shown in Fig. 1, is essentially the same as in the previous experiments [3], except that here water is injected vertically downwards through a copper tube (I.D. 11.1 mm). The perforated plate contains 15 10.5-mm holes, giving a porosity of 0.423. The pool overflow is located 267 mm above the test plate. The water that penetrates through the plate is drained through the bottom outlet. The steam is injected downwards at a 45° angle to minimize entrance effects, and can flow out either with the water overflow or the steam outlet at the top of the channel.

Four heights of water injection above the test plate were employed: 356, 203, 51 and 0 mm. The water jet was directed towards the hole shown as shaded in the figure, except for the 0-mm case, when the tube was attached to the center hole. The water temperature varied between 0 and 12°C, and the mass flow rate from 0.023 to 0.491 kg s^{-1}. The steam was saturated, with a mass flow rate between 0.0074 and 0.0312 kg s^{-1}.

The zero-delivery point for a given inlet water flow rate is here defined as the point where downward liquid delivery just begins. It was determined visually by gradually increasing the steam flow rate until no delivery is observed through the plate. For the two lowest water injection heights, the water jet penetrated through the perforated plate before being turned around. In this case, zero-delivery corresponds to a negligible rate of change in the level of water accumulated at the bottom of the channel. The total-delivery point, on the other hand, is defined as the point where the steam flow rate just fails to maintain the water pool above the plate, so that a sudden collapse of the pool is observed.

DATA CORRELATION

For the correlation of countercurrent gas–liquid vertical flow, the Wallis [4] or Kutateladze [5] models have been employed. An interpolative scaling between these two has been given by Bankoff *et al.* [3] in the form:

$$H_g^{*1/2}/C + H_f^{*1/2}/C = 1. \quad (1)$$

The dimensionless flow rates are defined by:

$$H_i^* = [\rho_i/gw(\rho_f - \rho_g)]^{1/2} j_i; \quad i = \text{f or g}, \quad (2)$$

where j_i is the volumetric flux of the ith phase, and w is a length scale given by:

$$w = D_h^{(1-\alpha)}[\sigma/g(\rho_f - \rho_g)]^{\alpha/2}. \quad (3)$$

Geometrical effects are taken into account by choosing α to be of the form:

$$\alpha = \tanh(2\pi D_h R/t_p), \quad (4)$$

where D_h is the hole diameter, R is the porosity of the plate and t_p is the plate thickness. Following the correlation obtained by

* This work was supported by a contract with the U.S. Nuclear Regulatory Commission.
† To whom communications should be addressed.